

Temperature dependence of giant tunnel magnetoresistance in epitaxial Fe/MgO/Fe magnetic tunnel junctions

S. G. Wang,^{1,2} R. C. C. Ward,^{1,*} G. X. Du,² X. F. Han,² C. Wang,³ and A. Kohn³

¹*Department of Physics, Clarendon Laboratory, University of Oxford, Oxford OX1 3PU, United Kingdom*

²*State Key Laboratory of Magnetism, Beijing National Laboratory for Condensed Matter Physics, Institute of Physics, Chinese Academy of Sciences, Beijing 100190, China*

³*Department of Materials, University of Oxford, Oxford OX1 3PH, United Kingdom*

(Received 22 August 2008; published 17 November 2008)

The temperature dependence of giant tunnel magnetoresistance (TMR) in epitaxial Fe/MgO/Fe magnetic tunnel junctions has been investigated. The resistance in the parallel configuration between the bottom (free) Fe layer and the top Fe layer, exchange biased by an IrMn antiferromagnetic layer, is nearly independent of the temperature. In contrast, in the antiparallel configuration the resistance increases with decreasing temperature, resulting in an increase in the TMR ratio from 170% at room temperature to 318% at 10 K. The dynamic conductance ($G' = dI/dV$) in the parallel configuration shows flat bias voltage dependence in the range ± 0.4 V, but in the antiparallel configuration it shows typical parabolic behavior as a function of bias voltage. A model, based on the temperature dependence of magnetic disorder in the two electrodes and its effect on the spin-dependent tunneling, is proposed to describe the temperature dependence of the TMR ratio and the resistance, in good agreement with our experimental data.

DOI: 10.1103/PhysRevB.78.180411

PACS number(s): 75.70.-i, 85.75.-d, 75.30.Cr

The magnetic tunnel junction (MTJ) is a key element of next generation spintronic devices such as magnetic random access memory and magnetic sensors. Following theoretical predictions^{1,2} of huge tunnel magnetoresistance (TMR) in epitaxial Fe/MgO/Fe junctions, measured TMR ratios about 200% at room temperature (RT) have been reported in MgO-based MTJs³⁻⁵ using Fe or Fe-alloy electrodes. Although epitaxial structures will probably not be used in devices, they remain excellent model systems to compare theoretical calculations and experimental results and to enhance our understanding of the spin-dependent tunneling.⁴⁻⁷

The TMR ratio (defined as $\frac{R_{AP}-R_P}{R_P} = \frac{G_P-G_{AP}}{G_{AP}}$, where $R_{P,AP}$ and $G_{P,AP}$ is the resistance R and static conductance $G = I/V$ in the parallel (P) and antiparallel (AP) configurations, respectively) exhibits both bias voltage and temperature dependences, which play critical roles in device applications. For bias voltage dependence, the dramatic decrease in the TMR ratio at relatively low bias has been attributed to magnon and phonon excitations in both AlO_x-based and MgO-based MTJs.^{8,9} In order to explain the temperature dependence of the TMR ratio of AlO_x-based MTJs, the Julliere model¹⁰—which relates the TMR ratio to the spin polarization of the electrodes—has been modified to include a spin-independent tunneling term.¹¹⁻¹³ Importantly, the TMR ratio as a function of temperature was well described in a simple phenomenological model in which spin polarization was taken to decay according to the Bloch law in the same way as magnetization.¹² A similar model was applied to sputtered polycrystalline MgO-based MTJs.¹⁴ For epitaxial Fe/MgO/Fe MTJs,¹⁵ it was explained in principle by scattering-driven interfacial contributions to the spin-polarized tunneling of the minority spin channel in the AP configuration compared with the majority spin channel tunneling in the P configuration, which has less temperature dependence. However, a characteristic feature of high-quality MgO barrier is that R_P is almost independent of temperature and low bias

voltage,^{3,6,9} while R_{AP} decreases significantly with temperature, resulting in the observed decrease in the TMR ratio by a factor of ≈ 2 between 10 and 300 K (this factor is lower for Co and CoFe electrodes). It is concluded from theoretical considerations^{16,17} that the direct application of the Julliere expression for the TMR ratio is not appropriate to the case of spin-dependent tunneling. The flat temperature and bias dependences of R_P , which have been attributed to the high band gap (8 eV) of MgO,⁹ are certainly not predicted by the Julliere theory. Despite these reservations, the Julliere theory has been utilized recently to evaluate the temperature dependence of the TMR ratio in epitaxial Co/MgO/Co junctions.⁶ However, to date there has been no quantitative model proposed for the detailed temperature dependences of the TMR ratio in epitaxial MgO-based MTJs.

Here, we analyze the temperature dependences of TMR ratio, $R_{P,AP}$, and dynamic conductance, in fully epitaxial Fe/MgO/Fe/IrMn MTJs, where a single Fe layer and an Fe/IrMn exchange-biased bilayer are used as the bottom (free) and top electrode (pinned), respectively. R_P is indeed found to be nearly temperature independent, while R_{AP} increases significantly with decreasing temperature, leading to an increase in the TMR ratio from 170% at RT to 318% at 10 K. This is among the highest TMR values measured in epitaxial Fe/MgO/Fe MTJs.^{4,5} Based on the relationship between spin-polarized tunneling across the barrier and the magnetic disorder of the electrodes as a function of temperature, a model is proposed with a good quantitative explanation of experimental results.

Fully epitaxial Fe/MgO/Fe/IrMn structures, together with reference samples of single Fe layer and Fe/Ir_{0.2}Mn_{0.8} bilayers (Fe/IrMn), were grown on MgO(001) substrates by molecular beam epitaxy. The epitaxial relationship Fe(001)[100]/MgO(001)[110]/Fe(001)[100]/IrMn(001)[110] is found with sharp interfaces; further details can be found elsewhere.^{18,19} Junctions ($6 \times 8 \mu\text{m}^2$ in size, 36 per sample)

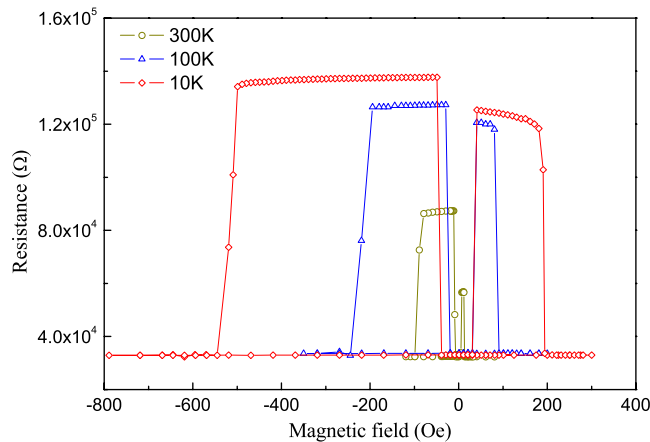


FIG. 1. (Color online) Resistance as a function of the magnetic fields at temperatures of 300, 100, and 10 K in MTJs of structure Fe(25)/MgO(3)/Fe(10)/IrMn(10) (thickness in nm). The field is parallel to the [100] easy axis of the Fe and Fe/IrMn bilayer.

were patterned by optical lithography combined with Ar-ion beam milling. The magnetotransport properties were measured in a physical properties measurement system with a magnetic field applied parallel to the Fe[100] easy axis. Magnetic measurements of the single Fe layer and Fe/IrMn bilayer were carried out using a superconducting quantum interference device magnetometer (Quantum Design); the diamagnetic contribution of MgO substrate was subtracted. Dynamic conductance $G' = dI/dV$ was obtained by a standard lock-in method at 23 Hz with a modulation voltage of 1 mV.²⁰

Two junctions (labeled Junction-1 and Junction-2) from one sample with structure of Fe(25)/MgO(3)/Fe(10)/IrMn(10) (thicknesses in nm) are selected. Figure 1 shows typical R - H loops at 300, 100, and 10 K for Junction-1. It shows low and high resistance in the P and AP configurations, respectively. A TMR ratio of 170% is found at RT and increases to 318% at 10 K, and its temperature dependence will be analyzed in detail below. It shows that the coercivity and the exchange bias field in the Fe/IrMn bilayers both increase markedly with decreasing temperature. This is a much stronger temperature dependence than that reported by other groups^{4,6} and is attributed to the full epitaxial nature of the structures here, in contrast to the sputtered IrMn layers employed elsewhere.

Figure 2(a) shows the resistances of Junction-1 in the P and AP configurations as functions of temperature (solid dots and open dots, respectively). R_P is seen to be nearly independent of temperature, while R_{AP} increases monotonically with decreasing temperature. The temperature dependence of the TMR ratio is shown in Fig. 2(b) for Junction-1 and Junction-2 by open diamonds and open circles, respectively. With increasing temperature, the TMR ratio exhibits an approximately linear decrease, in agreement with results from other groups.^{3,15} However, we find a reproducible departure from linearity of the TMR ratio vs T relationship, and the solid lines in Fig. 2(b) are fits based on the model to be described below. The dependence of the dynamic conductance G'_P and G'_{AP} on bias voltage in the junction with struc-

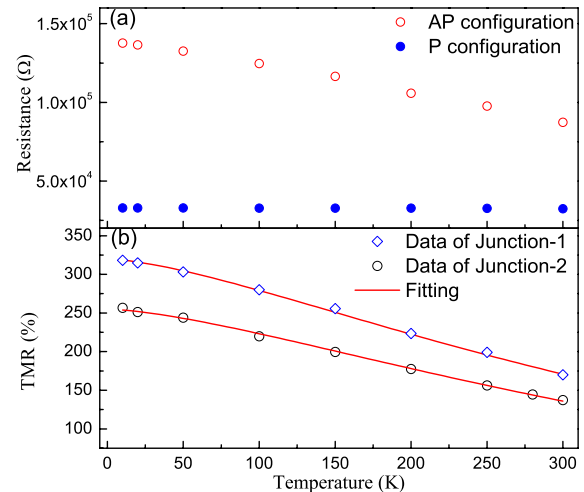


FIG. 2. (Color online) (a) Resistance in the P (solid dots) and AP (open dots) configurations as a function of temperature. (b) Temperature dependence of TMR ratio for two junctions. Solid lines are fits based on Eq. (4).

ture of Fe(50)/MgO(2)/Fe(10)/IrMn(10) (thickness in nm) has been measured at low and room temperatures, and the results are shown in Fig. 3. The parallel conductance exhibit flat bias dependence in the range ± 0.4 V at both 10 and 300 K, again a characteristic of high-quality MgO barrier.⁹ In contrast, G'_{AP} shows a typically parabolic shape with a zero-bias anomaly, which has been attributed to magnon and/or phonon excitations. Furthermore, at low bias voltages, G'_P decreases between 10 and 300 K, while G'_{AP} increases.

The spin-dependent tunneling in epitaxial Fe/MgO/Fe junctions has been described in detail by first-principles theory.^{16,17} A single-crystal MgO barrier exhibits a spin filtering effect due to the conservation of wave-function symmetry. The conductance in P configuration, dominated by majority Δ_1 states, is high because Δ_1 states decay relatively slowly through the barrier and can transfer into similar-symmetry states in the second electrode. By contrast, the conductance in AP configuration is symmetry blocked. Un-

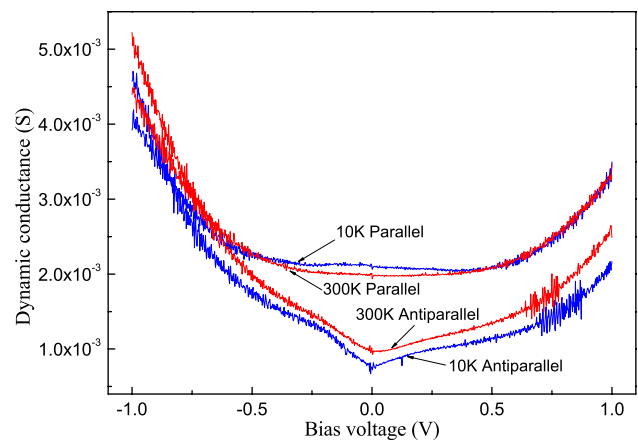


FIG. 3. (Color online) Dynamic conductance ($G' = dI/dV$) as a function of bias voltage in P and AP configurations at 300 and 10 K, where the MTJs have Fe(50)/MgO(2)/Fe(10)/IrMn(10) (thickness in nm) structure.

fortunately, the first-principles theory cannot take the temperature dependence into account. Furthermore, the calculations assume that the electrode magnetizations are ideally collinear. We propose that the symmetry blocking in the AP configuration will become less effective if the magnetizations of two electrodes are noncollinear. The perturbation of magnetization alignment of the electrodes is considered to be the dominant effect on the temperature dependence of the TMR ratio, and its effect on R_{AP} is much greater than that on R_P . In order to develop a model for detailed temperature dependence of the TMR ratio in epitaxial MgO-based MTJs, we use as a starting point an expression for the conductance of a tunnel junction first introduced by Slonczewski:²¹ $G = G_0(1 + P_1 P_2 \cos \theta)$, where P_1 and P_2 are the effective spin polarizations of the ferromagnetic (FM) electrodes and θ is the angle between their magnetizations. Our reasons for using a free-electron-type model are: (i) the observation¹⁷ that Slonczewski's description of the TMR ratio agrees fairly well with full first-principles calculations for the case of thicker barriers such as ≥ 2 nm used in our study, and (ii) the fact that, as yet, first-principles theories have considered only exactly collinear P and AP configurations.

In our empirical formulation, the definition of G given above is now modified by replacing polarization with magnetization and introducing individual angular terms to define the direction of electrode magnetizations with respect to the applied magnetic field. This step of the introduction of individual angular terms for the P and AP states is the main difference from previous models for AlO_x (Ref. 12) and sputtered MgO (Ref. 14) devices, and enables the TMR dependence of epitaxial MgO devices to be described fully without the introduction of a spin-independent tunneling component. The close link between polarization and magnetization has been mentioned by previous authors^{22–24} and references therein. Our model assumes that polarization is directly proportional to magnetization in the case of bcc Fe.²⁴ Experimentally, the saturation magnetization of an FM layer as a function of temperature can be taken as a measure of the magnetic disorder, and its temperature dependence is well described by thermal excitation of spin waves at temperatures far below the Curie temperature with Bloch's law:²⁵

$$M_{1,2}(T) = M_{1,2}^0(1 - \alpha T^{3/2}). \quad (1)$$

Here, α is a material-dependent constant and $M_{1,2}^0$ denotes the saturation magnetizations of two magnetic layers at $T = 0$ K. This law has been experimentally confirmed for bulks, thin films, and surface magnetization; the latter is important for MTJs because tunneling is an extremely surface-sensitive process.¹² The $M(T)$ curves for 25-nm-thick Fe layer and the Fe/IrMn bilayer are shown in Fig. 4. The measurements were carried out in an applied magnetic field of 1000 Oe between 10 and 370 K. Good agreement between the data points and Bloch's law is found with values of $\alpha = 7.0 \times 10^{-6}$ and 9.2×10^{-6} ($\text{K}^{-3/2}$) [together with $M_{1,2}^0 = 2.14 \times 10^{-3}$ and 9.29×10^{-4} (emu), respectively] extracted from the fits (solid lines in Fig. 4) for 25 nm Fe layer and Fe(10 nm)/IrMn(10 nm) bilayer, respectively. These values are typical for Fe layers and show the enhancement of spin-wave excitations with decreasing thickness.²⁵

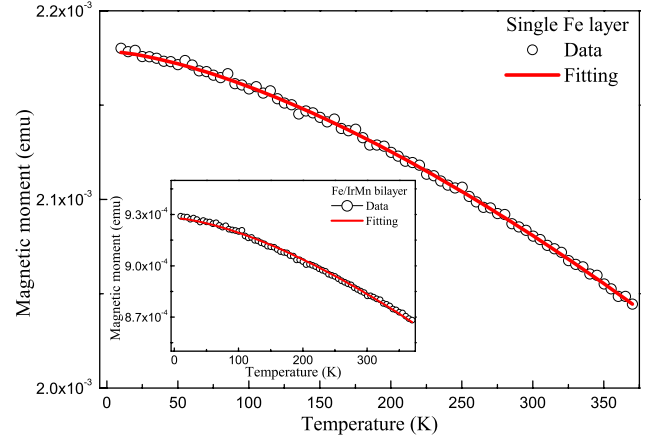


FIG. 4. (Color online) Saturation magnetization of an Fe layer (25 nm thick) as a function of temperature. Inset: $M(T)$ curve for an Fe(10 nm)/IrMn(10 nm) bilayer. Solid lines are fits based on Eq. (1).

For bcc bulk Fe, there are Δ_1 , Δ_5 , and Δ_2' states for majority spins, and Δ_5 , Δ_2 , and Δ_2' , without Δ_1 states due to exchange splitting for the minority spins, respectively. Based on above discussion, the temperature dependence of conductance is expressed in terms of the magnetizations of two electrodes and their angles θ_1 and θ_2 with respect to the direction of applied magnetic field. For P configuration, $G_P(T, \theta) = G_P^0[1 + \beta_P M_1^0 M_2^0 \cos(\theta_1 - \theta_2)]$, where the parameter β_P is closely related to the majority of Δ_1 states, which dominate the conductance in P configuration. For AP configuration, we get $G_{AP}(T, \theta) = G_{AP}^0[1 - \beta_{AP} M_1^0 M_2^0 \cos(\theta_1 + \theta_2)]$, where β_{AP} is only related to the other states except Δ_1 , such as Δ_5 and $\Delta_{2,2}'$, because an injected Δ_1 states cannot find equivalent symmetry in the opposite FM electrode with reversed magnetization in AP configuration. Furthermore, $\beta_{P,AP}$ includes the proportionality factor relating spin polarization and magnetization and also takes account of the local interface effect on the spin-polarized electron tunneling. In the temperature range investigated here, the angle $\theta_{1,2}$ with respect to applied magnetic field is very small, confirmed by Bloch's law shown in Fig. 4. Therefore, $G_{P,AP}$ could be further simplified as

$$\begin{cases} G_P(T, \theta) = G_P^0[1 + \beta_P M_1^0 \cos \theta_1 M_2^0 \cos \theta_2] \\ G_{AP}(T, \theta) = G_{AP}^0[1 - \beta_{AP} M_1^0 \cos \theta_1 M_2^0 \cos \theta_2] \end{cases}. \quad (2)$$

Finally we get

$$\begin{cases} G_P(T) = G_P^0[1 + \beta_P M_1(T) M_2(T)] \\ G_{AP}(T) = G_{AP}^0[1 - \beta_{AP} M_1(T) M_2(T)] \end{cases}. \quad (3)$$

The saturation magnetization described by Bloch law exhibits a little decrease with temperature shown in Fig. 4, leading to a decrease in G_P (increase in R_P) and an increase in G_{AP} (decrease in R_{AP}) with increasing temperature.

Now, the TMR ratio can be expressed as

$$\text{TMR} = \frac{G_P^0 [1 + \beta_P M_1^0 M_2^0 (1 - \alpha_1 T^{3/2})(1 - \alpha_2 T^{3/2})]}{G_{AP}^0 [1 - \beta_{AP} M_1^0 M_2^0 (1 - \alpha_1 T^{3/2})(1 - \alpha_2 T^{3/2})]} - 1. \quad (4)$$

The fits by Eq. (4) are shown by the solid lines in Fig. 2(b), in good agreement with the experimental data. It should be emphasized that the fitting was carried out using the values of $\alpha_{1,2}$, which were obtained from the fitting of the $M(T)$ curves of the Fe layer and Fe/IrMn bilayers. The parameter $\beta_{P,AP}$ is defined as above, its value $\beta_{P,AP} M_1^0 M_2^0 = 0.190$ and 0.907 for Junction-1, and $\beta_{P,AP} M_1^0 M_2^0 = 0.195$ and 0.911 for Junction-2 from fitting, respectively. The small deviation is coming from the local structures at the interfaces. The value of β_P is much smaller than that of β_{AP} , indicating the misalignment due to thermal effect plays a much more effective role on G_{AP} than on G_P . Theoretical results also find the primary effect of thermal disorder is to significantly increase G_{AP} while G_P is much less affected.¹⁷ The fitting of the TMR ratio vs T has been repeated successfully for different junctions with MgO barrier thicknesses of 2 and 3 nm and with bottom Fe layer thickness of 25 and 50 nm. We conclude that the temperature dependences of the TMR ratio in epitaxial MgO-based junctions are well described by our model, where the very different temperature dependences of G_P and G_{AP} are explained by the effectively greater misalignment of

magnetizations in the AP configuration, when responding to thermally driven magnetic disorder. The ferromagnetic coupling of the two electrodes at barrier thicknesses ≥ 0.8 nm tends to maintain collinearity of the magnetizations in the P state.¹⁵ The sensitivity of the TMR ratio to changes in the magnetic band structure of the electrodes as a function of temperature was emphasized previously in calculations, based on Slonczewski's model, of ideal Co/I/Co junctions.²³ The present model offers a physical interpretation of this effect in terms of misalignments of the magnetizations in the two electrodes. Small change in magnetization alignment leads to large changes in the TMR ratio.

In summary, the temperature dependence of the TMR ratio in epitaxial Fe/MgO/Fe MTJs has been investigated. An empirical model based on the misalignment of magnetizations in the electrodes due to thermal excitations and its effect on the spin-dependent tunneling across the barrier has been proposed. The model provides a good fit to the experimental data, well describing the nonlinear dependence of the TMR ratio between 10 K (318%) and room temperature (170%).

We are grateful to X.-G. Zhang at Oak Ridge National Laboratory for helpful comments, to Keith Belcher for technical support, and to the Engineering and Physical Sciences Research Council (EPSRC-GB) for financial support.

*Corresponding author: Roger.ward@physics.ox.ac.uk

¹W. H. Butler, X.-G. Zhang, T. C. Schulthess, and J. M. MacLaren, *Phys. Rev. B* **63**, 054416 (2001).

²J. Mathon and A. Umerski, *Phys. Rev. B* **63**, 220403(R) (2001).

³S. S. Parkin, C. Kaiser, A. Panchula, P. M. Rice, B. Hughes, M. Samant, and S. H. Yang, *Nature Mater.* **3**, 862 (2004).

⁴S. Yuasa, T. Nagahama, A. Fukushima, Y. Suzuki, and K. Ando, *Nature Mater.* **3**, 868 (2004).

⁵C. Tiusan, J. Faure-Vincent, C. Bellouard, M. Hehn, E. Jouguelet, and A. Schuhl, *Phys. Rev. Lett.* **93**, 106602 (2004); R. Guerrero, D. Herranz, F. G. Alieva, F. Greullet, C. Tiusan, M. Hehn, and F. Montaigne, *Appl. Phys. Lett.* **91**, 132504 (2007).

⁶S. Yuasa, A. Fukushima, H. Kubota, Y. Suzuki, and K. Ando, *Appl. Phys. Lett.* **89**, 042505 (2006).

⁷D. Waldron, V. Timoshevskii, Y. Hu, K. Xia, and H. Guo, *Phys. Rev. Lett.* **97**, 226802 (2006).

⁸X. F. Han, J. Murai, Y. Ando, H. Kubota, and T. Miyazaki, *Appl. Phys. Lett.* **78**, 2533 (2001).

⁹G. X. Miao, K. B. Chetry, A. Gupta, W. H. Butler, K. Tsunekawa, D. Djayaprawira, and G. Xiao, *J. Appl. Phys.* **99**, 08T305 (2006).

¹⁰M. Julliere, *Phys. Lett.* **54A**, 225 (1975).

¹¹L. Yuan, S. H. Liou, and D. X. Wang, *Phys. Rev. B* **73**, 134403 (2006).

¹²C. H. Shang, J. Nowak, R. Jansen, and J. S. Moodera, *Phys. Rev. B* **58**, R2917 (1998).

¹³M. Oogane, J. Nakata, H. Kubota, Y. Ando, A. Sakuma, and T.

Miyazaki, *Jpn. J. Appl. Phys., Part 2* **44**, L760 (2005).

¹⁴X. Kou, J. Schmalhorst, A. Thomas, and G. Reiss, *Appl. Phys. Lett.* **88**, 212115 (2006).

¹⁵J. Faure-Vincent, C. Tiusan, E. Jouguelet, F. Canet, M. Sajjeddine, C. Bellouard, E. Popova, M. Hehn, F. Montaigne, and A. Schuhl, *Appl. Phys. Lett.* **82**, 4507 (2003); J. Faure-Vincent, C. Tiusan, C. Bellouard, E. Popova, M. Hehn, F. Montaigne, and A. Schuhl, *Phys. Rev. Lett.* **89**, 107206 (2002).

¹⁶J. M. MacLaren, X. G. Zhang, and W. H. Butler, *Phys. Rev. B* **56**, 11827 (1997).

¹⁷W. H. Butler, X.-G. Zhang, S. Vutukuri, M. Chshiev, and T. C. Schulthess, *IEEE Trans. Magn.* **41**, 2645 (2005).

¹⁸S. G. Wang, G. Han, G. H. Yu, Y. Jiang, C. Wang, A. Kohn, and R. C. C. Ward, *J. Magn. Magn. Mater.* **310**, 1935 (2007).

¹⁹C. Wang, S. G. Wang, A. Kohn, R. C. C. Ward, and A. K. Petford-Long, *IEEE Trans. Magn.* **43**, 2799 (2007).

²⁰X. F. Han, A. C. C. Yu, M. Oogane, J. Murai, T. Daibou, and T. Miyazaki, *Phys. Rev. B* **63**, 224404 (2001).

²¹J. C. Slonczewski, *Phys. Rev. B* **39**, 6995 (1989).

²²J. S. Moodera, J. Nowak, and R. J. M. van de Veerdonk, *Phys. Rev. Lett.* **80**, 2941 (1998).

²³A. H. Davis, J. M. MacLaren, and P. LeClair, *J. Appl. Phys.* **89**, 7567 (2001).

²⁴M. Beth Stearns, *J. Magn. Magn. Mater.* **5**, 167 (1977).

²⁵W. Kipferl, M. Dumm, M. Rahm, and G. Bayreuther, *J. Appl. Phys.* **93**, 7601 (2003).